Characterization of model and real catalysts by APXPS

Virginia Pérez-Dieste[1*]

[1]ALBA Synchrotron Light Source, Carrer de la Llum 2-26, 08290, Cerdanyola del Vallès, Barcelona, Spain

Abstract. In this contribution, I first briefly summarize some of the recent advances relevant for the investigation of heterogeneous catalysis with Ambient Pressure X-ray Photoelectron Spectroscopy (APXPS). In the second part, two examples of the research done at the CIRCE beamline of the synchrotron ALBA are described: CO oxidation on a model curved crystal Pd(111) catalyst and methanol steam reforming on powder bimetallic supported catalysts, PdCu/ monoclinic and cubic zirconia.

1 Introduction

Ambient Pressure XPS typically refers to XPS performed with pressures at the sample of up to a few (~20) mbar, as opposed to standard XPS, for which the analysis chamber needs to be kept in ultra-high vacuum.

Over the last two decades, this technique has earned a place in the repertoire of prominent spectroscopies for in-situ characterization of catalysts' surfaces. A turning point in the development of APXPS was the design by Ogletree et al. in 2002 [1], in which the differential pumping system of the photoelectron analyser, already present in earlier designs, was upgraded with a set of electrostatic lenses to focus the photoelectrons through the small apertures between the pumping stages, significantly increasing the count rate and enabling routine operation at a few mbar.

The distinctive feature of APXPS is the surface and interface sensitivity for operando studies of the electronic structure. The fields of application can be classified according to interface type as those involving solid-gas and solid-vapor interfaces, which comprise heterogeneous catalysis, electrocatalysis, electrodes and batteries in air, wetting, corrosion,… solid-liquid interfaces, including electrified solid-liquid interfaces, and liquid-gas interfaces, with the focus on environmental chemistry.

The information that can be obtained includes the evolution of the oxidation state and chemical environment of surface atoms in reaction, segregation and strong metal support interaction phenomena, changes in the work function, depth profiling and ion distribution in electrified interfaces in operando. It is also possible to monitor the product distribution analysing the gas phase composition above the surface.

A good number of excellent APXPS reviews are available [1-10]. The aim of this contribution is to provide a brief look at some of the most recent advances relevant for heterogeneous catalysis, and to present two examples of APXPS experiments performed at the CIRCE beamline of ALBA.

1.1 Recent advances in APXPS for heterogeneous catalysis

As a relatively young technique, APXPS is evolving and diversifying at a fast pace. One of the explored routes is its simultaneous combination with other in-situ techniques, ensuring the same sample conditions and direct correlation of the information from both sources. Gas product characterization by mass spectrometry, proton transfer-reaction mass spectrometry, or gas chromatography allows to confirm that the reaction is taking place and to monitor activity and selectivity [11].

Ambient pressure Near Edge X-ray Absorption Fine Structure spectroscopy in total and partial electron yield modes is almost by defect available at synchrotron setups, and it gives access to the unoccupied electronic structure of surfaces. Varying the X-ray polarization or its incidence angle, it can be used to determine a preferential orientation of adsorbed gas molecules.

Vibrational spectroscopies like Infrared Reflection Absorption Spectroscopy (IRRAS) and Polarization Modulated-IRRAS are now available at a few synchrotron and lab APXPS setups, and they can be used to ascertain the bonding geometry and adsorption site of gas molecules in model catalysts, or to characterize the active site location and properties by means of titration experiments [12-14].

Recently, APXPS has also been combined with grazing incidence X-ray scattering (GIXS) [15]. Wide and small angle GIXS provide respectively atomic and mesoscopic scale (~200nm) dynamic (µs) structural information that can be correlated with the chemical evolution monitored by APXPS.

In the last few years there has been an impressive progress in the development of time resolution methods for APXPS, key to address the dynamics of catalytic processes.

* Virginia Pérez-Dieste: vperezdieste@cells.es

The hundreds of ms range is already accessible in 3rd and 4th generation synchrotrons directly using the fast, snapshot, mode of MCP/CCD or delay line detectors [8,16]. Essential areas and phenomena like chemical kinetics, detection of short-lived surface intermediates, spectators and active phase identification, segregation or nanoparticle restructuring can be tackled.

To make good use of the time-resolution, a perturbation is needed in order to drive the system out of equilibrium and make the event of interest take place at a larger rate than its opposite. Knudsen et al. have used periodical gas pulses as perturbation, combined with lock-in plus image recognition analysis to achieve a time resolution of 60 ms with very good signal to noise ratio for reversible and repetitive processes [17].

In their method, time resolved data are recorded continuously in snapshot mode during several periodical perturbation cycles and a feature that signals a phase transition on the surface (new species, work function change, etc) is chosen as the locking signal. In this way, the response to each pulse does not need to be exactly the same to be able to add data to accumulate statistics, as the corresponding spectra can be aligned in time using the lock-in signal, detected by the image recognition software. Weak surface and gas phase components simultaneously present can be unveiled and correlated, while preserving the time resolution. The phase transitions during CO oxidation on Pd(100) at 3 mbar and 100 mbar were mapped with down to 60 ms resolution and it was shown that all the surface phases: thick oxide, "Ö5" oxide and CO covered metallic phase, were active to some degree.

Shavorskiy et al. have developed a pump and probe scheme that can reach 20 µs resolution, at the Hippie beamline in Max IV [16]. A fast valve is used to create ms gas pulses in the mbar range. The valve actuator is synchronized with the opening of a shutter on the electron analyzer detector fast camera through a delay generator that allows recording data only at the selected delay. Performing measurements at increasing delays, the time-dependent evolution of the APXPS spectra can be monitored for the whole gas pulse. This scheme also requires that the catalyst response to the gas pulse be reproducible.

The method was applied to the CO oxidation reaction on Pt(111) and it was shown that the higher CO_2 production occurs for PO2/PCO=0.9-2.3, when the surface contains both chemisorbed oxygen and surface oxides, which was interpreted as indication that both the Langmuir-Hinshelwood and the Mars-van-Krevelen mechanisms intervene in the reaction.

Redekop et al. have implemented the gas pulse perturbation approach at the Species beamline in Max IV using a time counting, delay-line detector. In this proof-of-concept work, emphasis has been put on the careful characterization of the gas transport within the cell during the pulses, obtaining an estimation of the residence time and of the intrinsic reaction rate constant range that can be accessed [18].

Last—and the least in the race against the clock—Favaro et al. have reported achieving 30 ns time resolution with good statistics and energy resolution in a new APXPS endstation using a 3D delay line detector [19].

Another pending task in the APXPS evolution is closing the remaining pressure gap among tenths of mbar operation and industrial catalytic conditions, usually above 1 bar. Since 2019, the 1 bar milestone can be efficiently reached at the Polaris instrument in Dessy, using tender X-rays to increase the photoelectron mean free path and optimizing all the rest of parameters: sample to nozzle distance, nozzle aperture, sample position stability, analyzer transmission, … [20]. The surface sensitivity (~10Å) can be preserved exploiting grazing incidence geometry (~0.05º-1º). Depth profiling in a large range (~10-150Å) is possible by sweeping the angle, and even larger depths can be reached by increasing the photon energy. For example, it was shown that the Pd(100) surface adopts an island structure during CO_2 oxidation at 300 mbar, with metallic islands growing on top of oxide islands [21].

The Polaris setup uses the gas beam dosing approach, consisting of creating a local high pressure area at the sample position while maintaining the background pressure in high vacuum [22]. This strategy is useful for gas-pulse time-resolved experiments, as it allows a fast exchange of the gas in the high pressure region [17]. The routine operation pressure is currently in the 300-500 mbar range, although 2.5 bar can be reached.

Blomberg et al. showed the potential of this instrument to explore a wide pressure range, obtaining a global picture of the pressure dependence of surface species, products and intermediates, in a Pd(100) surface during CO oxidation with diluted gases [23]. More recently, other reactions of high practical interest, like the Fisher-Tropsch reaction on Fe(110) and the CO_2 hydrogenation on Zn/ZnO/Cu(211) have been addressed [24-25].

2 APXPS for heterogeneous catalysis at ALBA

Model heterogeneous catalysts with usually simple and known structures facilitate experimental reproducibility and admit first-principles calculations closer to the experimental configuration, both things favoring solid understanding of partial processes. On the other hand, more realistic, oxide supported, diluted, multimetallic, structurally defective, multiphase… catalysts preserve most of the complex and dynamic interactions among their components. Next, two examples of APXPS studies, for model and realistic catalysts, both for relatively simple reactions, are summarized.

2.1 CO oxidation in curved Pd(111)

The CO oxidation reaction has been extensively examined by APXPS as a model reaction in model catalysts, in mono and bimetallic supported nanoparticles, in oxides nanorods,… [4]. In this work a Pd(111) curved crystal was used [26]. Curved crystals contain a collection of vicinal surfaces; therefore they represent an intermediate case between single crystals

and nanoparticles, and allow studying a variety of crystallographic planes with different atomic coordination sites in a single experiment, in the same experimental conditions.

The c-Pd(111) was exposed to a 1:1 $CO:O_2$, 0.15 mln/min flow at P=0.6 mbar, at 370 K. The temperature was increased up to 570 K, and then decreased to 470 K. The sample was scanned with the 100 x 20 μm^2 beam, probing the different vicinals with an angle step of 2°. At 570 K the whole surface was active, as indicated by the CO_2 production and the absence of adsorbed CO. In Fig. 1, the C1s and O1s spectra for T=485 K during cooling-off are shown.
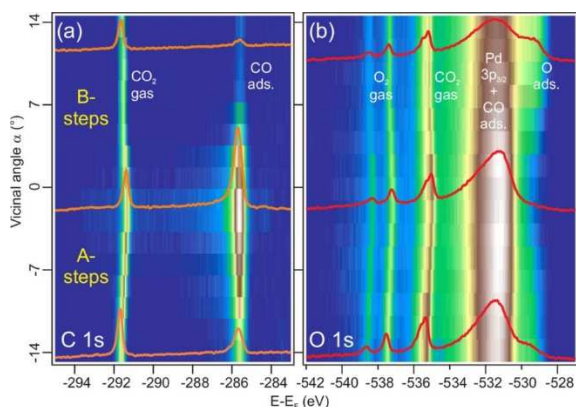

Fig. 1. C1s (a) and O1s (b) intensity plots across the curved surface at 485K, during reaction cooling-off. In (a), the strong variation of the chemisorbed CO indicates that the reaction is poisoned at the sample center, becoming more active towards the A side and fully active at the B edge. Reprinted with permission from [26]. Copyright (2018) American Chemical Society.

The co-adsorbed CO intensity is maximum at the Pd(111) (α=0°) and it decreases with increasing vicinal angle, more markedly towards the B-type (111) steps direction. The O1s intensity exhibits a complementary variation, with an additional feature at BE=529 eV assigned to chemisorbed oxygen and surface and sub-surface oxides. Then, at 485K the catalytic oxidation of CO is switched off at the (111) surface, but it is still ongoing at highly stepped crystal planes and the B-type steps are more active than the A-type steps. At 570 K the oxides are present also in the (111), however at 485 K they only persist in highly stepped vicinals, indicating that they are more difficult to reduce. Their presence could also be favoured by the gas mixture becoming locally more oxidizing when the sample region is CO depleted [23] .

2.2 PdCu/ZrO₂ for methanol steam reforming

In this work we investigated Pd-Cu bimetallic catalysts supported on zirconia for the methanol steam reforming (MSR) reaction to produce H_2 [27]. Methanol is liquid at room temperature, what makes it easy to transport, and it is a well suited fuel for H_2 production due to its high H/C ratio and because it does not have C-C bonds, which leads to a lower reforming temperature than for other alcohols .

Cu-based catalysts are the most used for MSR due to their high activity and selectivity to H_2 and their low CO production and cost. However, they have low thermal stability and deactivate easily. To minimize that problem, they are usually supported on oxides and co-catalysts are added. Pd is a good candidate because it presents good thermal stability and relatively low CO selectivity. The metal loading was 20% Cu and 4% Pd.

Two different catalysts with monoclinic and cubic zirconia were prepared and the fixed bed reactor catalytic tests indicated that the catalyst with monoclinic ZrO_2 had higher catalytic activity, higher methanol conversion (90% vs. 40% at 240ºC) and lower CO production (5% vs. 20% at 240ºC) than the one with cubic zirconia support. The goal of the study was trying to explain the origin of such performance differences.

The X-Ray Diffraction and Scanning Electron Microscopy results revealed that the metal dispersion was better in the monoclinic catalyst, with a mean Cu crystal size ~2 times smaller than in the cubic catalyst.
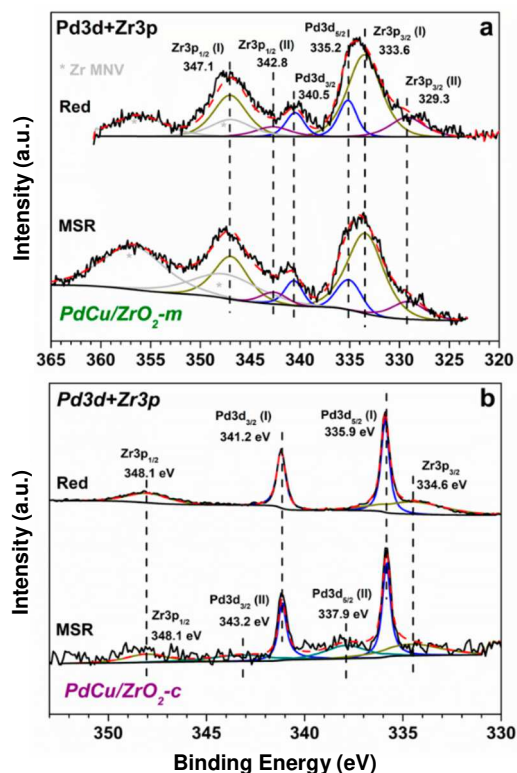

Fig. 2. Pd3d+Zr3p core levels acquired with hν=500eV in reducing and MSR conditions in monoclinic (a) and cubic (b) ZrO_2 supported catalysts. Reproduced from [27]

For the APXPS experiments, the powder samples were pressed into pellets and first pre-treated at 1 mbar H_2 and 300ºC for 2 hours to clean and reduce the metals. Then APXPS during the MSR reaction was performed at 1mbar CH_3OH: H_2O 2:3 at T=180 ºC

In Fig. 2, the Pd 3d plus Zr 3p spectra in reduction and during the MSR reaction are shown. In the monoclinic catalyst two ZrO_2 components are present both in reduction and in reaction, assigned to different oxidation states, probably Zr^{+4} and Zr^{+3}. On the other hand, in the cubic catalyst the Zr component is very weak and only one component was identified, assigned to Zr^{4+}.

In the cubic catalyst the Pd is in metallic state during reduction and in reaction there is a small oxide component. In the monoclinic catalyst the Pd $3d_{3/2}$ appears at lower binding energy than the metallic Pd, what could be due to PdCu alloying.

The Pd/Zr atomic ratio was calculated from the data and a 15 times lower value was found for the monoclinic catalyst than for the cubic one, which indicates a better dispersion of the metals in the catalyst surface. From the area ratio change, it is also deduced that in the cubic catalyst the Pd segregates towards the surface during MSR, while for the monoclinic catalyst Pd is stable.

Then, it was concluded that the cubic sample presented metal agglomeration, surface oxidation and metal segregation towards the surface under working conditions. In contrast, PdCu alloy is probably present in the monoclinic catalyst, preventing in that case the oxidation under reaction conditions. In addition, the metal distribution is stable during reaction in the monoclinic catalyst and it presents a mixture of oxidation states with vacants that can promote water activation. The good dispersion of the active phase also contributes to the observed enhanced MSR activity.

XPS experiments with realistic catalysts are often hindered by charging of the oxide support. Zirconia, for example, is a large band gap material, ~5 eV, but this experiment was feasible thanks to the relatively large metal loading and to the presence of gas in APXPS, which helps discharging [10]. Other tricks to minimize charging are making the pellets as thin as possible, making the pellets sandwiching a thin Au mesh, or measuring near to the usually metallic sample clamp. Heating and a reducing pre-treatment may also help. Nevertheless, some peak broadening could not be totally excluded in this case, maybe favoured by sample inhomogeneity. Surface spectromicroscopy with moderated spatial resolution has been used to check and correct the effects of an inhomogeneous sample potential, making studies with complex catalysts more accessible [28].

In the current global context, rational optimization of industrial catalytic processes is necessary as part of a sustainable energy roadmap, and it can be affirmed that APXPS is quickly developing in the right directions to contribute to this challenge.

Acknowledgments

References

1. D.F. Ogletree, H. Bluhm, E.D. Hebenstreit and M. Salmeron, Nucl. Instrum. Methods Phys. Res. A, **601,** 151 (2009)

2. H. Bluhm, J. Electron Spectrosc. Relat. Phenom.*,* **177,** 71 (2010)

3. D. E. Starr, Z. Liu, M. Hävecker, A. Knop-Gericke, and H. Bluhm, Chem. Soc. Rev. **42**, 5833 (2013).

4. J. Schnadt, J. Knudsen, and N. Johansson, J. Phys.: Condens. Matter **32**, 413003 (2020).

5. *"Ambient Pressure Spectroscopy in Complex Chemical Environments"* (A. R. Head, S. Nemsák and B. Eren, ACS Symp. Series, 2021)

6. W. R. Flawell, R.S. Chemistry. (2022) DOI: 10.1039/d2fd00071g

7. S. Zafeiratos, T. Dintzer, D. Teschner et al. J. Catal., **269**, 309 (2010)

8. K. Roy, L. Artiglia and J.A. van Bokhoven *ChemCatChem* **10** 666 (2018)

9. Y. Han, H. Zhang, Y. Yu, and Z. Liu, ACS Catal., **11**, 1464, (2021)

10. R. Dupuy, C. Richter, B. Winter et al. J. Chem. Phys. **154**, 060901 (2021)

11. A.V. Bukhtiyarov, I. P. Prosvirin, M. A. Panafidin et al. Nanomat., **11**, 3292 (2021)

12. A. R. Head, O. Karslioğlu, T. Gerber et al. Surface Science **665,** 51 (2017)

13. K. I. Hadjiivanov, G. N. Vayssilov, Adv. Catal. **47**, 307 (2002)

14. K. Mudiyanselage, D. J. Stacchiola, "In-situ *Characterization of Heterogeneous Catalysts"*, (John Wiley & Sons, Inc., 2013, pp. 209)

15. H. Kersell, P. Chen, H. Martins et al., Rev. Sci. Inst. **92**, 044102 (2021)

16. A. Shavorskiy, G. D'Acunto, V. Boix de la Cruz et al. ACS Appl. Mater. Interfaces, **13**, 47629 (2021)

17. J. Knudsen, T. Gallo, V. Boix et al. Nat. Commun., **12**, 6117 (2021)

18. E. A. Redekop, N. Johansson, E. Kokkonen, et al. Rev. Sci. Instrum., **92**, 044101 (2021)

19. M. Favaro, P.C.J. Clark, M. J. Sear, Surf. Sci. **713,** 121903 (2021)

20. P. Amann, D. Degerman, M.-T. Lee et al. Rev. Sci. Instrum., **90**, 103102 (2019)

21. C.M. Goodwin, M. Shipilin, S. Albertin, J. Phys. Chem. Lett. **12** 18, 4461 (2021)

22. J. Pantförder, S. Pöllmann, J. F. Zhu Rev. Sci. Inst. **76**, 014102 (2005)

23. S. Blomberg, U. Hejral, M. Shipilin, et al., ACS Catal., **11**, 9128 (2021)

24. M. Shipilin, D. Degerman, P. Lomker, ACS Catal. **12**, 7609 (2022)

25. P. Amann; B. Klotzer, D. Degerman, Science, **376**, 6593, 603 (2022)

26. F. Schiller, M. Ilyn, V. Pérez-Dieste, et al., J. Am. Chem. Soc., **140**, 16245 (2018)

27. D. Ruano, B.M. Pabón, C. Azhenha et al. Catalyst **10**, 1005 (2020)

28. P. Bargiela, V. Fernandez, C. Cardinaud et al. Appl. Surf. Sci., **566**, 150728 (2021)